Electronic Supplementary Material (ESI) for Soft Matter.

Supporting Information for

A model of cell-wall dynamics during sporulation in *Bacillus subtilis*

L. W. Yap[‡a] and R. G. Endres[ab]
[a] *Department of Life Sciences, Imperial College, London, United Kingdom.*
[b] *Centre for Integrative Systems Biology and Bioinformatics, Imperial College, London, United Kingdom.*
[‡] *Present address: Department of Biosystems Science and Engineering (D-BSSE), ETH Zürich, Switzerland*

ADDITIONAL RESULTS FOR MINIMAL MODEL

Effects of membrane synthesis

To study the effect of membrane synthesis on the cell wall, we extended the minimal model, to include the membrane surface areas (Fig. S1a). The forespore membrane surface area $A_s^{mb} = 4\pi r^2$ is constant, whilst the mother cell membrane surface area $A_m^{mb} = 4\pi r^2 + 2\pi rL + 4\pi r^2 \sin\theta$ increases with engulfment. All other parameters from the original model were retained, with the forespore and mother cell wall surface areas re-written as A_s^{cw} and A_m^{cw}, respectively. The membrane also contributes a bending energy, which, at $4.14 \cdot 10^{-8}$ MPa μm^3 [S1], is approximately 10^7 times smaller than the cell wall bending energy [S2] and thus can be neglected. The energy equation now reads:

$$E = -p_m V_m - p_s V_s + (\gamma - \varepsilon)(A_m^{cw} + A_s^{cw}) + (\gamma_2 - \varepsilon_2)(A_m^{mb} + A_s^{mb}) + 2\pi r_s f + E_m^{bend} + E_s^{bend}, \tag{5}$$

with membrane surface tension γ_2 and chemical potential ε_2 for membrane synthesis. Since we are interested in the partial derivative of E with respect to θ, we can rewrite Eq. (5) as:

$$E \approx (\gamma - \varepsilon) \cdot A_s^{cw} + 2\pi f \cdot r_s \, + \, E_s^{bend} + (\gamma_2 - \varepsilon_2) \cdot A_m^{mb} \tag{6}$$

The dynamic equation for engulfment is:

$$\left(\eta_\theta^{cw} V_\theta^{cw} + \eta_\theta^{mb} V_\theta^{mb}\right)\left(\frac{\dot\theta}{\theta^2}\right) = -\frac{\partial E}{\partial \theta} \tag{7}$$

with membrane viscosity constant $\eta_\theta^{mb} = 1/(2\pi h \mu_\theta^{mb})$. We estimated the membrane mobility coefficient μ_θ^{mb} to be significantly higher than that of the cell wall, so the viscosity constant of the membrane is negligible. Finally, $\gamma_2 = 0.1\ nN/\mu$m [S1], which is 10^3 times smaller than the cell wall surface tension [S2] and hence can also be ignored. Thus, using Eq. (6) in Eq. (7), we obtain:

$$\frac{\partial E}{\partial \theta} = (\gamma - \varepsilon) \cdot 2\pi r^2 \cdot \cos\theta - 2\pi r f \cdot \sin\theta \, + \, 4k_s \pi r^2 \Big(\frac{1}{r} - \frac{1}{R_0}\Big)^2 \cdot \cos\theta + -2\varepsilon_2 \cdot 2\pi r^2 \cdot \cos\theta \tag{8}$$

Finally, we assumed that the chemical potentials for synthesizing the cell wall and membrane are the same, i.e. $\varepsilon = \varepsilon_2$:

$$\frac{\partial E}{\partial \theta} = (\delta - 2\varepsilon) \cdot 2\pi r^2 \cdot \cos\theta - 2\pi r f \cdot \sin\theta \, + \, 4k_s \pi r^2 \Big(\frac{1}{r} - \frac{1}{R_0}\Big)^2 \cdot \cos\theta \tag{9}$$

with $\delta = \gamma - \varepsilon$. As a result, the phase diagram in the dimensionless $(\tilde\delta - 2\tilde\varepsilon)$, $\tilde f$ plane (Fig. S1b) is identical to that in the $(\tilde\delta,\, \tilde f)$ plane of the original model (Fig. 3c). Assuming positive $\tilde\varepsilon$, the value of $\tilde\delta$ in the ordinate axis of the original phase diagram (Fig. 3c) is effectively reduced.

Effects of cell size

As individual cells may vary in size (though this size variation is limited [S3]), we plotted the change in the engulfment angle θ against time for varying r and fixed $\tilde\delta$ and $\tilde f$ in the absence of membrane synthesis (Fig. S1c). (Note that variation of L does not affect engulfment dynamics because L does not occur in the ODE for $\theta(t)$.) We found that deviation of r from the preferred radius R_0 has limited effect on the plot for $\theta(t)$.

Effects of elastic strain

We also considered the case in which the cell wall has not only plastic but also elastic properties [S4]. In addition to the surface tension γ already present in Eq. (2) of the main text, we considered cell-wall elasticity [S5], which is proportional to $(A_m^{cw} + A_s^{cw})^2$ and has coefficient γ_0, with $\gamma_0/\gamma \leq 0.1$:

$$E = -p_m V_m - p_s V_s + (\gamma - \varepsilon)(A_m^{cw} + A_s^{cw}) + \gamma_0 (A_m^{cw} + A_s^{cw})^2 + 2\pi r_s f + E_m^{bend} + E_s^{bend}, \tag{10}$$

which gives:

$$\frac{\partial E}{\partial \theta} = (\delta - 2\varepsilon) \cdot 2\pi r^2 \cdot \cos\theta - 2\pi r f \cdot \sin\theta + \gamma_0 (2\pi r^2)^2 \cdot \sin 2\theta \tag{11}$$

The resulting ensemble plots for $\tilde{\delta}$ and $\tilde{f}$ (Figs. S1d-e) are almost identical to the ensemble plots in the main text for which elastic strain was not considered (Figs. 2a-b). This shows the limited impact of elastic strain on engulfment in our model.

Effects of bending energy of septum

As the septum and forespore cell wall are initially assumed to be a single PG layer [S6] and thus 20 times as thin as the mother-cell wall [S2, S7], we assumed that $\tilde{k}_s$ is 20 times smaller than $\tilde{k}_m = 3.6$. Hence, the rescaled circumferential bending energy of the forespore cell wall $\tilde{k}_s$ was chosen to be 0.18. We found that, under the effect of the bending energy of the septum, deviation of r from the preferred radius R_0 slows down completion of engulfment, but the overall shape of the plot for $\theta(t)$ remains unchanged (Fig. S1f). Hence, for deviation of r by $\leq 5\%$, the contribution of $\tilde{k}_s$ to engulfment is indeed minor.

DETAILS FOR REALISTIC MODEL

Here, we provide further details for the realistic model, for which the septum is initially flat. For $q_2 = l$, we obtain:

$$\frac{dl}{dt} = -\mu_l \cdot \frac{l^2 \cdot \left\{ \frac{2}{3}\pi r^2 \Delta p + \delta \pi r \cdot \left[\sin^{-1}\left(\sqrt{1-\frac{r^2}{l^2}}\right) \cdot \left(\frac{1}{\sqrt{1-\frac{r^2}{l^2}}} - \frac{r^2}{l^2\left(\sqrt{1-\frac{r^2}{l^2}}\right)^3} \right) + \frac{r}{l\left(1-\frac{r^2}{l^2}\right)} \right] \right\}}{r^2 \left[1 + \frac{l}{r\sqrt{1-\frac{r^2}{l^2}}} \cdot \sin^{-1}\left(\sqrt{1-\frac{r^2}{l^2}}\right) \right]}, \tag{12}$$

where $\mu_l = 1/(\pi h \eta_l)$ is the mobility coefficient of forespore expansion.

For $q_3 = r$, we obtain:

$$\begin{aligned} \frac{dr}{dt} = \frac{\mu_r}{1 + \frac{l}{r\sqrt{1-\frac{r^2}{l^2}}} \cdot \sin^{-1}\left(\sqrt{1-\frac{r^2}{l^2}}\right) + 2\sin\theta + 4\pi + 2\pi\frac{L}{r}} \cdot \Bigg\{ -p_m\left(2\pi r^2 + 2\pi r L - \frac{4}{3}\pi r l\right) - p_s\left(\frac{4}{3}\pi r l + 2\pi r^2\right) \\ + \delta \cdot \left[10\pi r + 2\pi L + 4\pi r \sin\theta + \sin^{-1}\left(\sqrt{1-\frac{r^2}{l^2}}\right) \cdot \left(\frac{\pi l}{\sqrt{1-\frac{r^2}{l^2}}} + \frac{\pi r^2}{l^2\left(\sqrt{1-\frac{r^2}{l^2}}\right)^3} \right) - \frac{\pi r}{1-\frac{r^2}{l^2}} \right] \\ + 2\pi f \cdot \cos\theta + k_m \cdot \left[\pi L \left(\frac{1}{R_0^2} - \frac{1}{r^2} \right) + \frac{16\pi}{R_0}\left(\frac{r}{R_0} - 1\right) \right] \Bigg\}, \end{aligned} \tag{13}$$

where $\mu_r = 1/(\pi h \eta_r)$ is the mobility coefficient of radial growth.

For $q_4 = L$, we obtain:

$$\frac{dL}{dt} = \mu_L \cdot \frac{L}{r} \cdot \left[p_m(\pi r^2) - 2\delta\pi r - k_m \pi \left(\frac{1}{r} - \frac{2}{R_0} + \frac{r}{R_0^2} \right) \right], \tag{14}$$

where $\mu_L = 1/(2\pi h \eta_L)$ is the mobility coefficient of longitudinal growth.

Whilst most parameters are defined by single-cell imaging [S2], others such as the mobility coefficients must be estimated for our numerical model calculations. The mobility coefficient of engulfment ($\mu_\theta = 1\, m^2 J^{-1} h^{-1}$)

TABLE I: Model parameters

Symbol	Parameter	Value	Ref.	Notes
μ_θ	Mobility coefficient of engulfment	$1\, m^2 J^{-1} h^{-1}$	See text	
p	Turgor pressure	1.5 MPa	[S2, S8]	
R_0	Preferred radius of cell-wall cross-section	0.43 μm	[S2]	
r	Initial radius of *B. subtilis*	0.43 μm	[S2]	
$\tilde{\gamma} = \gamma/(pR_0)$	Rescaled surface tension		[S2]	
$\tilde{\varepsilon} = \varepsilon/(pR_0)$	Rescaled chemical potential		[S2]	
$\tilde{\delta} = \tilde{\delta} - \tilde{\varepsilon}$	Diff. b/w surface tension and chem. potential	-0.5 to 0.5	[S2]	Varied
$\tilde{f} = f/(pR_0^2)$	Rescaled line tension	-0.2 to 0.2	[S2]	Varied
$\tilde{k}_m = k_m/(pR_0^3)$	Rescaled bending rigidity of mother-cell wall	3.6	[S2]	
$\tilde{k}_s = k_s/(pR_0^3)$	Rescaled bending rigidity of forespore cell wall	0.18	See text	
μ_l	Mobility coefficient of forespore expansion	$55\, m^2 J^{-1} h^{-1}$	See text	
L	Initial length of *B. subtilis*	3.4 μm	[S9]	
$\Delta p = p_m - p_s$	Pressure diff. b/w mother cell and forespore	-0.1 MPa	[S1, S10]	
μ_r	Mobility coefficient of radial growth	$4 \cdot 10^{-2}\ m^2 J^{-1} h^{-1}$ $2\, m^2 J^{-1} h^{-1}$	See text	Limited growth Significant growth
μ_L	Mobility coefficient of longitudinal growth	$4 \cdot 10^{-3}\ m^2 J^{-1} h^{-1}$ $4 \cdot 10^{-2}\ m^2 J^{-1} h^{-1}$	See text	Limited growth Significant growth
dt	Time step	$0.01\, h$	[S6]	

is estimated to be significantly lower than that of forespore expansion ($\mu_l = 55\, m^2 J^{-1} h^{-1}$), suggesting that engulfment experiences a stronger opposing frictional force than forespore expansion. This could be because the leading edge of the engulfment membrane pushes against and helps remodeling the solid peptidoglycan cell wall, whereas the forespore expands and pushes against the semi-fluid cytoplasm of the mother cell, which may offer lower resistance. Table S1 shows the values of the various parameters used in the minimal and realistic models, as well as their sources.

With the initial assumption of no mother-cell growth, we plotted ensemble plots for the shape degrees of freedom θ and l for a range of $\Delta p = p_m - p_s$ (Figs. S2a-b). As evident from Eq. (4) in the main text, $\theta(t)$ does not depend on Δp, so the same plot is produced for all values of Δp (Fig. S2a). The ensemble plot for $l(t)$ shows that l remains constant for ≥ 100 seconds before increasing sharply to $L/2$ (Fig. S2b).

Finally, with the assumption of mother-cell growth, we plotted ensemble plots for the shape degrees of freedom θ, l, r, and L for a range of $\Delta p = p_m - p_s$ (Figs. S3 and S4). The plot for $l(t)$ with either significant or limited growth are similar compared to without growth. The plot for $\theta(t)$ with growth also shows similar dynamics compared to without growth before engulfment is complete, with the exception of engulfment not being able to complete if Δp is too negative, e.g. -0.3 MPa (Fig. S3a). After engulfment is complete, the predicted plots for $\theta(t)$ actually tend towards $\theta_2^* = \tan^{-1}\left[(r\tilde{\delta} + 2r\tilde{k}_s(1/r - 1/R_0)^2)/\tilde{f}\right]$, but this might not be biologically relevant as the migrating membrane fuses. When engulfment is not yet complete, the ensemble plots for $r(t)$ and $L(t)$ are in fact similar to the original framework, with $r(t)$ increasing and reaching a plateau, and $L(t)$ increasing linearly [S2]. If Δp is too negative, especially for significant mother-cell growth, we predict abnormal behaviour in the form of a sudden increase in $r(t)$ (Figs. S3c and S4c) and fluctuations in $L(t)$ (sudden shrinkage in Fig. S3d).

—

[S1] Ojkic, N., J. López-Garrido, K. Pogliano, and R. G. Endres. 2014. Bistable forespore engulfment in Bacillus subtilis by a zipper mechanism in absence of the cell wall. *PLoS Comput. Biol.* 10:e1003912.

[S2] Banerjee, S., N. F. Scherer, and A. R. Dinner. 2016. Shape dynamics of growing cell walls. *Soft Matter.* 12:3442-3450.

[S3] Chien, A. C., N. S. Hill, and P. A. Levin. 2012. Cell size control in bacteria. *Curr. Biol.* 22:R340-349.

[S4] Amir, A., F. Babaeipour, D. B. McIntosh, D. R. Nelson, and S. Jun. 2014. Bending forces plastically deform growing bacterial cell walls. *Proc. Natl. Acad. Sci. USA.* 111:5778-5783.

[S5] Jiang, H., F. Si, W. Margolin, and S. X. Sun. 2011. Mechanical control of bacterial cell shape. *Biophys. J.* 101:327-335.

[S6] Ojkic, N., J. López-Garrido, K. Pogliano, and R. G. Endres. 2016. Cell-wall remodeling drives engulfment during Bacillus subtilis sporulation. *Elife.* 5:e18657.

[S7] Tocheva, E. I., J. López-Garrido, H. V. Hughes, J. Fredlund, E. Kuru, M. S. Vannieuwenhze, Y. V. Brun, K. Pogliano, and G. J. Jensen. 2013. Peptidoglycan transformations during Bacillus subtilis sporulation. *Mol. Microbiol.* 88:673-686.

[S8] Lan, G., C. W. Wolgemuth, and S. X. Sun. 2007. Z-ring force and cell shape during division in rod-like bacteria. *Proc. Natl. Acad. Sci.* 104:16110-16115.

[S9] Sharpe, M. E., P. M. Hauser, R. G. Sharpe, and J. Errington. 1998. Bacillus subtilis cell cycle as studied by fluorescence microscopy: constancy of cell length at initiation of DNA replication and evidence for active nucleoid partitioning. *J. Bacteriol.* 180:547-555.

[S10] Stragier, P. and R. Losick. 1996. Molecular genetics of sporulation in Bacillus subtilis. *Annu. Rev. Genet.* 30:297-341.

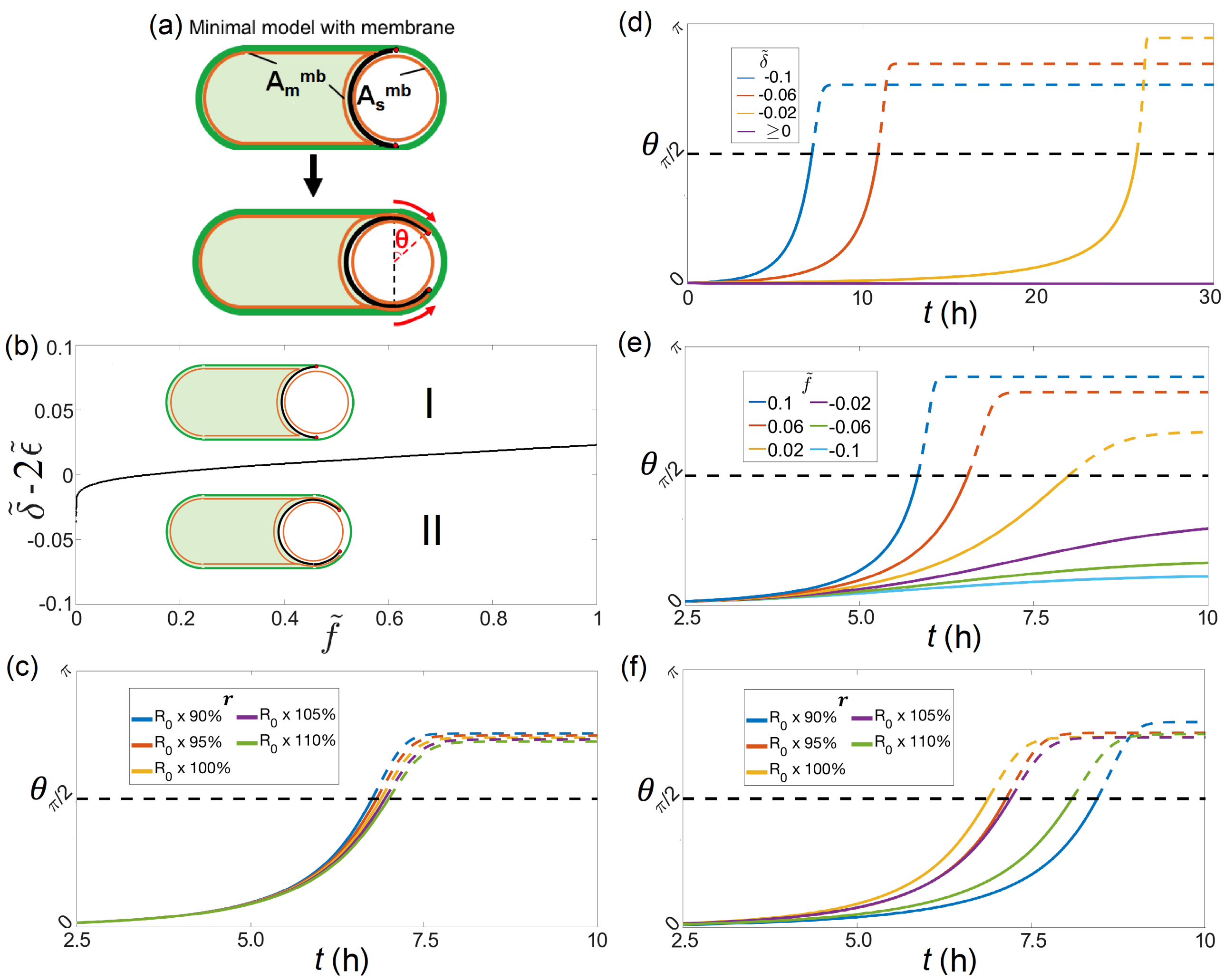

FIG. S1: **Additional results for minimal model of engulfment.** (a) Minimal model with membranes highlighted in orange. The forespore membrane surface area A_s^{mb} is constant, whilst the mother cell membrane A_m^{mb} increases with engulfment. (b) Phase diagram in the $(\tilde{\delta} - 2\tilde{\varepsilon}, \tilde{f})$ plane, with difference $\tilde{\delta} = \tilde{\gamma} - \tilde{\varepsilon}$ between surface tension and chemical potential, as well as line tension $\tilde{f}$. (c) Plot of $\theta(t)$ when initial cell radius r is varied in the absence of bending energy of septum, whilst $\tilde{\delta} = -0.1$ and $\tilde{f} = 0.04$ are kept constant. (d) Plot of $\theta(t)$ in presence of cell-wall elasticity ($\gamma_0/\gamma \leq 0.1$) when $\tilde{\delta}$ is varied, whilst $\tilde{f} = 0.04$ is kept constant. The plot is almost identical to Fig. 2a in the main text, where cell-wall elasticity is not considered. (e) Plot of $\theta(t)$ in presence of cell-wall elasticity ($\gamma_0/\gamma \leq 0.1$) when $\tilde{f}$ is varied, whilst $\tilde{\delta} = -0.1$ is kept constant. The plot is almost identical to Fig. 2b in the main text, where cell-wall elasticity is not considered. For all other parameters, see Table S1. (f) Plot of $\theta(t)$ when initial cell radius r is varied in the presence of bending energy of septum, whilst $\tilde{\delta} = -0.1$ and $\tilde{f} = 0.04$ are kept constant.

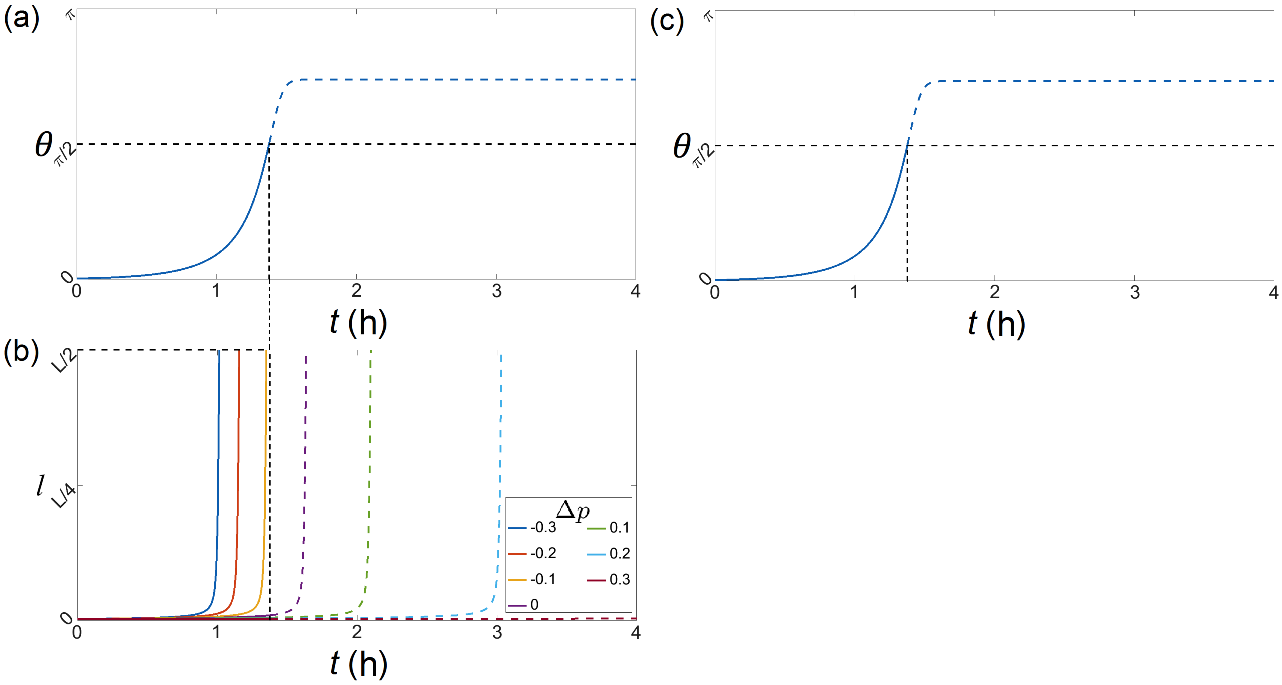

FIG. S2: **Ensemble plots of realistic model with $\mu_r = \mu_L = 0$ (no mother-cell growth).** (a) Plot of $\theta(t)$ for $-0.3 \leq \Delta p \leq 0.3$ MPa at fixed $\tilde{\delta} = -0.5$ and $\tilde{f} = 0.2$. The same plot is produced for all values of Δp, as $\theta(t)$ depends only on $\tilde{\delta}$ and $\tilde{f}$. (b) Plot of $l(t)$ when Δp is varied for fixed $\tilde{\delta} = -0.5$ and $\tilde{f} = 0.2$. Solid lines show forespore expansion during engulfment up to $\pi/2$, whereas dashed lines show forespore expansion if allowed to continue after engulfment is complete. Black dashed line represents time at which engulfment is complete. If $\Delta p < 0$ MPa, forespore expansion is completed before engulfment. For all other parameters, see Table S1. (c) Plot of $\theta(t)$ from minimal model for fixed $\tilde{\delta} = -0.5$ and $\tilde{f} = 0.2$, for comparison of engulfment dynamics between minimal (spherical forespore) and realistic (spheroidal forespore) models. The plot is the same as Fig. S2a, showing that, as differing only by forespore shape, both models yield nearly the same engulfment dynamics for the given set of parameter values.

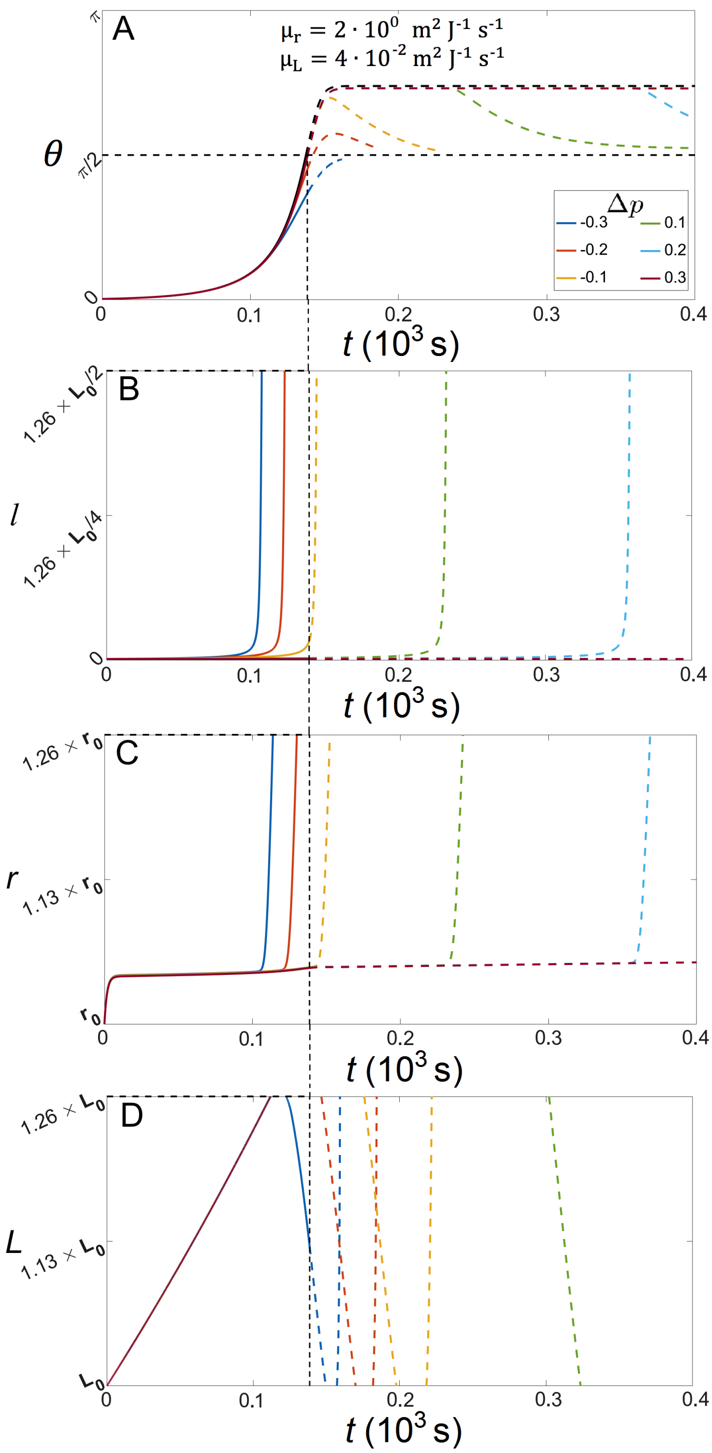

FIG. S3: **Ensemble plots of realistic model with significant mother-cell growth.** (a) Plot of $\theta(t)$ for different Δp in units of MPa. Black curve is the reference plot from Fig. S2a. Engulfment may not complete if Δp is too negative. (b) Plot of $l(t)$. Solid lines show forespore expansion during engulfment up to $\pi/2$, whereas dashed lines show forespore expansion if allowed to continue after engulfment is complete. Black dashed line represents time at which engulfment is complete. (c) Plot of $r(t)$. (d) Plot of $L(t)$. For all other parameters, see Table S1.

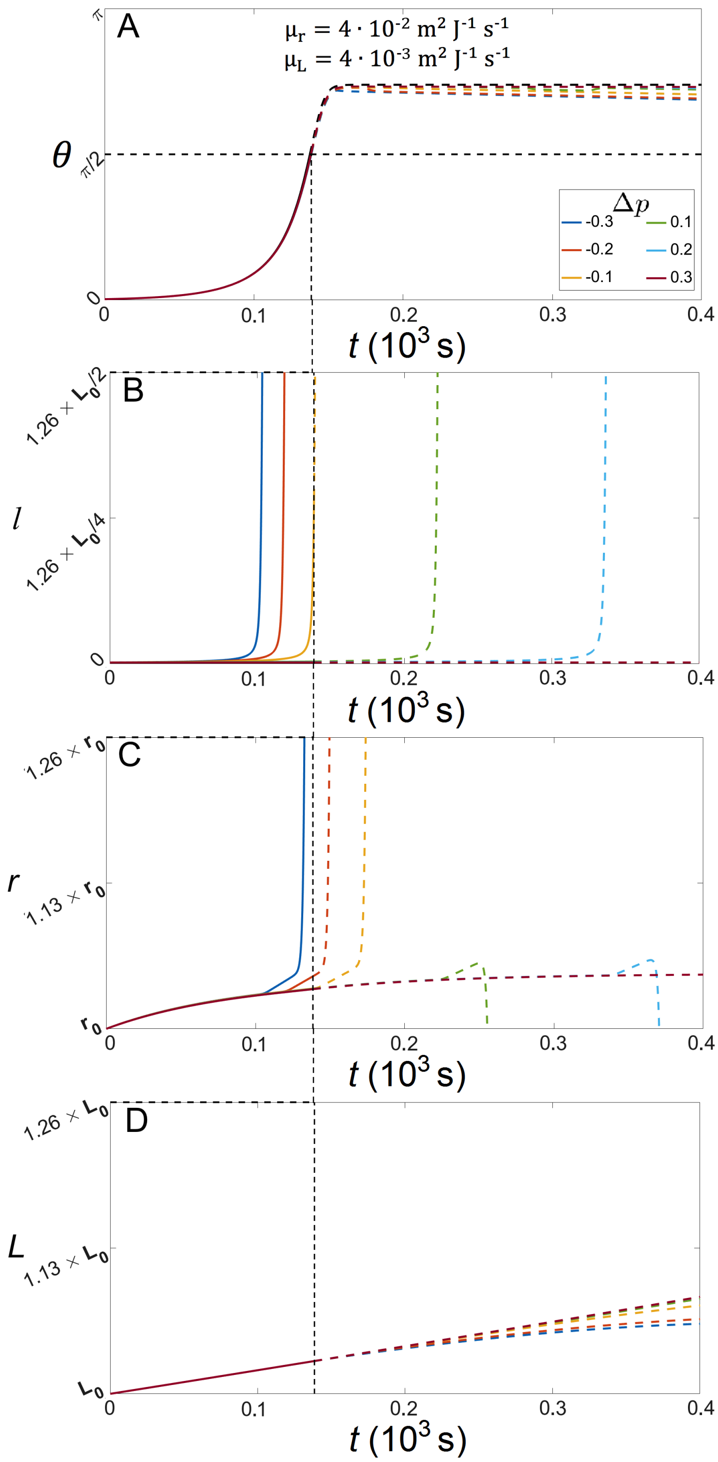

FIG. S4: **Ensemble plots of realistic model with limited mother-cell growth.** (a) Plot of $\theta(t)$ for different Δp in units of MPa. Black curve is the reference plot from Fig. S2a. (b) Plot of $l(t)$. Solid lines show forespore expansion during engulfment up to $\pi/2$, whereas dashed lines show forespore expansion if allowed to continue after engulfment is complete. Black dashed line represents time at which engulfment is complete. (c) Plot of $r(t)$. (d) Plot of $L(t)$. For all other parameters, see Table S1.